PHYSICAL REVIEW D **89,** 114023 (2014)

Improving combinatorial ambiguities of $t\bar{t}$ events using neural networks

Ji Hyun Shim and Hyun Su Lee*

Department of Physics, Ewha Womans University, Seoul 120-750, Korea

(Received 10 April 2014; published 25 June 2014)

We present a method for resolving the combinatorial issues in the $t\bar{t}$ lepton + jets events occurring at the Tevatron collider. By incorporating multiple information into an artificial neural network, we introduce a novel event reconstruction method for such events. We find that this method significantly reduces the number of combinatorial ambiguities. Compared to the classical reconstruction method, our method provides significantly higher purity with the same efficiency. We illustrate the reconstructed observables for the realistic top-quark mass and the forward-backward asymmetry measurements. A Monte Carlo study shows that our method provides meaningful improvements in the top-quark measurements using the same amount of data as other methods.

DOI: 10.1103/PhysRevD.89.114023 PACS numbers: 12.38.-t, 13.85.-t, 14.65.Ha

I. INTRODUCTION

The top quark was discovered in 1995 at the Fermilab Tevatron $p\bar{p}$ collider [1]. This recently discovered quark is the heaviest known elementary particle [2]. Its large mass may strongly couple with the electroweak symmetry breaking [3,4], and therefore the top quark is usually treated differently from the other light quarks in many new physics models. This suggests that many searches focus on the top quark signature [5]. Recent observations of the charge forward-backward asymmetry (A_{FB}) at the Tevatron collider may provide evidence for the involvement of this new physical signature in $t\bar{t}$ production [6,7]. However, because of the limited number of $t\bar{t}$ events at Tevatron, updated measurements using the full Tevatron data at the collider detector at Fermilab (CDF) still do not confirm whether they have identified a new physical signature or if the result is a statistical fluctuation of the standard model (SM) process [8]. Because the Large Hadron Collider (LHC) is a pp collider, it is difficult to probe all of the possible scenarios of new physics involved in the top-quark A_{FB}. It is, therefore, necessary to use the currently available Tevatron data as efficiently as possible.

Similar issues have occurred with the top-quark mass ($\mathrm{M_{top}}$) measurements. The top-quark mass is a fundamental parameter of the SM, and it is tightly related to the W-boson mass and Higgs-boson mass via electroweak radiative corrections [9,10]. Therefore, precision measurements of $\mathrm{M_{top}}$ and the W-boson indirectly provide important constraints on the Higgs boson mass. Compared with the directly-observed Higgs-boson mass [11], precision measurement of $\mathrm{M_{top}}$ can be important for understanding the SM. Even though LHC experiments obtained $t\bar{t}$ events that were more than two orders of magnitude larger than the Tevatron events, the Tevatron measurements give the most precise $\mathrm{M_{top}}$ results to date [12,13]. Because of the well-known detectors as well as the much smaller instantaneous luminosity of the collisions, the Tevatron measurements usually have smaller systematic uncertainties. Consequently, the dominant uncertainty of the Tevatron $\mathrm{M_{top}}$ measurement is statistical uncertainty [12], while the LHC measurement is dominated by systematic uncertainty [13]. Therefore, efficiently utilizing the currently available Tevatron data is important for improving the precision of Tevatron measurements as well as world average of $\mathrm{M_{top}}$.

In the SM, the top quark decays almost exclusively into a W boson and a b quark [2]. In $t\bar{t}$ events, the lepton + jets decay channel is defined by the case where one W boson decays leptonically into an electron or a muon plus a neutrino and the other W decays hadronically into a pair of jets. Thus, the events in this channel contain one charged lepton, two b quark jets, two light flavor quark jets, and one undetected neutrino. Many precise top-quark measurements including $\mathrm{M_{top}}$ and A_{FB} have been performed using lepton + jets events.

In the lepton + jets event, we have measured four final jets in the detector that should be matched with initial parton-level quarks. During event reconstruction, we should resolve these combinatorial ambiguities. The rate of correctly matching events for all four jets in the kinematic reconstruction method, which is commonly used in hadron collider experiments [14–17], was only 18%–47% depending on the b-tagging category after poorly reconstructed events were rejected by requiring that the minimum χ^2 be less than nine [14]. Other events use imperfect $t\bar{t}$ reconstruction from incorrect matching between jets and quarks. As shown in Ref. [14], incorrectly matching events resulted much poorer resolution in the distribution of observables such as the reconstructed top-quark mass and W-boson mass. If we develop an improved method for resolving the combinatorial ambiguities, the majority of the top-quark measurements can be significantly improved. In this paper, we report a novel

*hyunsulee@ewha.ac.kr

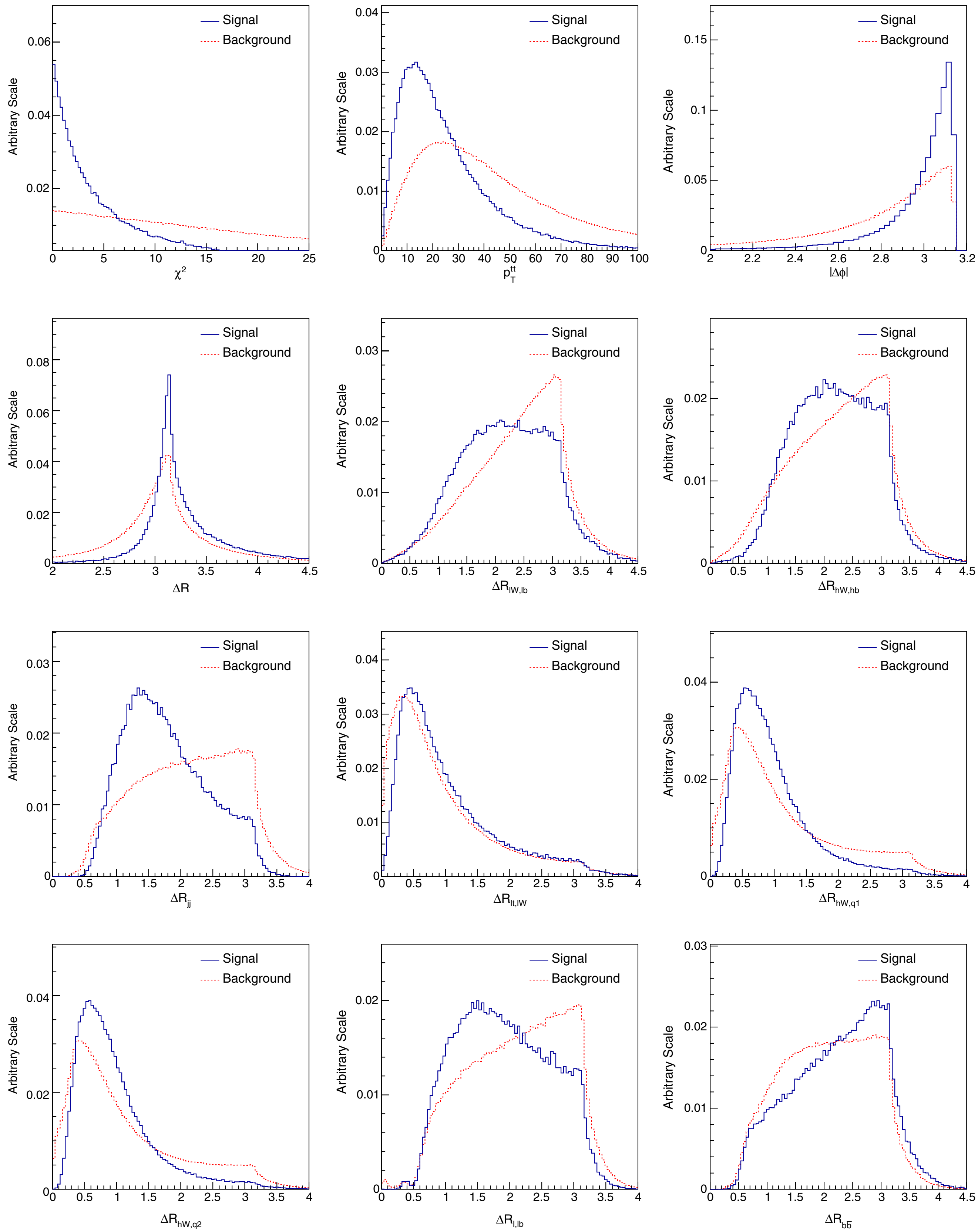

FIG. 1 (color online). Distributions of the neural network input variables for the M_{top} measurement of the signal (all jets are correctly matched) and the background (at least one jet unmatched) using a SM $t\bar{t}$ sample with $M_{top} = 173\ \mathrm{GeV}/c^2$.

technique for improving the combinatorial ambiguities of $t\bar{t}$ lepton + jets events using a multivariable neural network (NN) technique. This method is directly applicable to experimental measurements of the top quark such as M_{top} and A_{FB}.

There are a few studies that discuss the combinatoric ambiguities at hadron colliders [18–20]. However, these studies focus on new physics processes in pair production, and both particle and antiparticle decay into invisible particles that could be dark matter candidates. Therefore, the final state contains two invisible particles together with the visible particles. These methods can be directly applicable for the dilepton decay channel of $t\bar{t}$ events due to the two invisible neutrinos, but they are not feasible for lepton + jets decay events. Furthermore, those studies consider model-independent analysis because we may not exactly know what is underlying the new physics seen in the data. On the other hand, $t\bar{t}$ productions and decays are very precisely tested in the SM framework [2]. We can therefore use model-dependent analysis to maximize the information for resolving the combinatoric ambiguities. One very useful technique for incorporating multiple information is an artificial NN method [21,22]. Here, we propose the use of the artificial NN for resolving the combinatoric ambiguities in $t\bar{t}$ events.

II. $t\bar{t}$ EVENTS AND THEIR RECONSTRUCTION

For the study of $t\bar{t}$ event reconstruction, we generated a simulated $t\bar{t}$ signal sample with $M_{top} = 173\ \mathrm{GeV}/c^2$ [12,13] using the leading-order (LO) Monte Carlo (MC) generator MADGRAPH/MADEVENT [23] package with PYTHIA [24] parton showering. The detector effects are produced with the fast detector simulation package PGS [25]. The detector resolution effects are simulated by the following parametrization:

$$\frac{\delta E}{E} = \frac{a}{\sqrt{E}} \quad \text{for jets,} \qquad \frac{\delta E}{E} = \frac{b}{\sqrt{E}} \oplus c \quad \text{for leptons.}$$

As per the predefined values in the PGS package, we let $a = 0.8$, $b = 0.2$, and $c = 0.01$. The PGS package can also quickly reconstruct each physical object such as leptons, jets, and missing transverse energy. In the simulation, the jets originating from b quarks are tagged with approximately 40% b-tagging efficiency.

To select the candidate events in the $t\bar{t}$ lepton + jets channel, we require one charged lepton candidate with transverse momentum, p_T, greater than 20 GeV/c. We also require missing transverse energy ($\not{E}_T$) to exceed 20 GeV and at least four jets with transverse energy, E_T, greater than 20 GeV. We further request that at least one jet is tagged as a b quark.

We first attempt to reconstruct the $t\bar{t}$ lepton + jets events using the kinematic reconstruction method applied in the CDF analyses [14,26]. We build a χ^2 formula to obtain the most probable combination that combines all measured quantities and known constraints. Our method slightly differs from the CDF description in that we directly use $\not{E}_T$ instead of the unclustered energy with approximately 40% resolution because the unclustered energy is unavailable in the fast simulation. Therefore, we define χ^2 for the kinematic fit as follows:

$$\begin{aligned}\chi^2 = {} & \Sigma_{i=\ell,4\mathrm{jets}}(p_T^{i,\mathrm{fit}} - p_T^{i,\mathrm{meas}})^2/\sigma_i^2 \\ & + \Sigma_{k=x,y}(\nu_{T_k}^{\mathrm{fit}} - \not{E}_{T_k}^{\mathrm{meas}})^2/\sigma_k^2 \\ & + (M_{jj} - M_W)^2/\Gamma_W^2 + (M_{\ell\nu} - M_W)^2/\Gamma_W^2 \\ & + \{M_{bjj} - M_{\mathrm{top}}\}^2/\Gamma_t^2 \\ & + \{M_{b\ell\nu} - M_{\mathrm{top}}\}^2/\Gamma_t^2.\end{aligned}$$

In this χ^2 formula, the first term constrains the p_T of the lepton and the four leading jets to their measured values within their respective uncertainties (detector resolutions). The second term constrains both transverse components of $\not{E}_T$, x and y, as well as those of the neutrino, p_x and p_y. In the last four terms, the quantities M_{jj}, $M_{\ell\nu}$, M_{bjj}, and $M_{b\ell\nu}$ refer to the invariant masses of the four-vector sum of the particles denoted in the subscripts. Here, M_W and M_{top} are the masses of the W boson (80.4 GeV/c^2) [27] and the top quark, respectively, and M_{top} is determined during minimization of χ^2. The total widths of the W boson and the top quark are Γ_W (2.1 GeV/c^2) and Γ_t (1.5 GeV/c^2), respectively [2].

Assuming that the four leading jets in the detector are products of the $t\bar{t}$ decay, there are 12 possible jet-to-quark assignments. We perform a minimization for each assignment using a χ^2 comparison. In the classical kinematic reconstruction method (χ^2 method), the combination that has the lowest χ^2 is selected as a candidate for correctly matched events. To understand the performance of the reconstruction methods, we study the true quark properties together with the reconstructed jet properties. If the distance, $\Delta R \equiv \sqrt{(\Delta\eta)^2 + (\Delta\phi)^2}$, between a quark and a

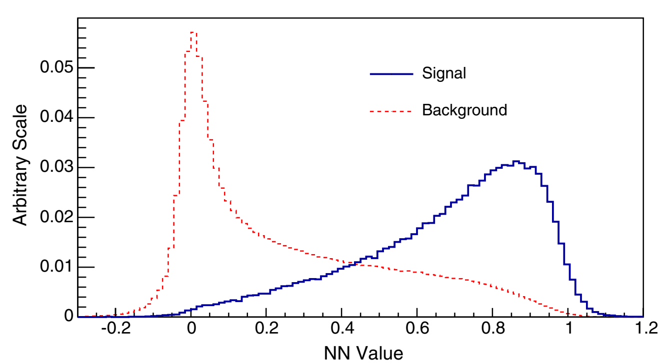

FIG. 2 (color online). Distribution of the neural network output for the M_{top} measurement of the signal and the background using a SM $t\bar{t}$ sample with $M_{top} = 173\ \mathrm{GeV}/c^2$.

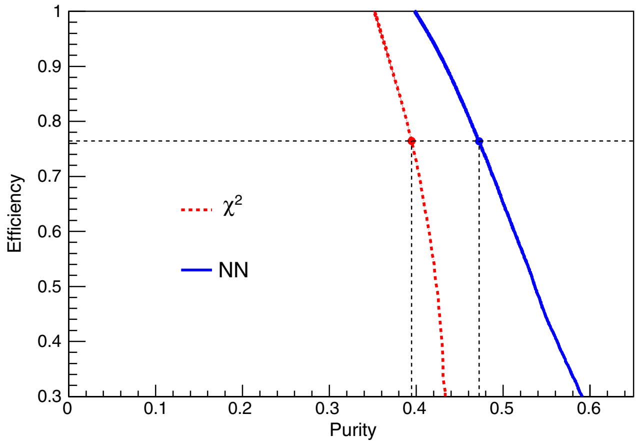

FIG. 3 (color online). The relationship between the purity and efficiency for the NN method and the χ^2 method is shown. At the same efficiency (76%), which corresponds to the $\chi^2 < 9$ cut, the NN method has 49% purity, while the χ^2 method has 39% purity.

reconstructed jet is less than 0.4, the jet-to-parton assignment is correct. If all four quarks and jets have correct assignments, this event has correct matching. We then obtain a purity, which is a fraction of the correct matching events, of 35% using the classical χ^2 method for the SM $t\bar{t}$ events. If we use the CDF requirement that χ^2 must be less than 9, which has an event efficiency of 76%, the purity is increased to 39%. The values of efficiency and purity are consistent with those in the CDF results [14].

Because there are 12 possible combinatorics, a purity about 35% is acceptable. Moreover, under our assumption that the four leading jets are candidates for the four quarks, the maximum purity of the SM $t\bar{t}$ sample is only 67%. However, without losing efficiency, the purity can be improved by up to 90% (35% → 67%). Even though χ^2 is important for matching the jets and quarks, there are many additional variables that can be used to determine the correctly matching combinations. Therefore, we employ the multivariable NN for the event reconstruction of $t\bar{t}$ lepton + jets events.

We use the results of the kinematic fitter for all possible combinatorics as the input for our neural network. Of the possible combinations, we choose a signal, which has all jets matched with the correct quarks, and background, where at least one jet is unmatched. We then train the NN with various kinematic input variables that have discrimination powers between the signal and the background. To avoid any measurement bias and to maximize the discrimination power, the choice of input variables depends on the measurements. The NN is constructed with the network implementation in the ROOT package [28].

III. $\mathrm{M_{top}}$ MEASUREMENT

For the $\mathrm{M_{top}}$ measurement, we consider kinematic variables that do not depend on $\mathrm{M_{top}}$ but have a discriminant power between the signal and the background. In addition to the χ^2 information, we consider the transverse momentum of the $t\bar{t}$ system $p_T^{t\bar{t}}$ as well as the azimuthal angle between the t and $\bar{t}$ quarks $\Delta\phi$ [29]. Without additional radiation, $p_T^{t\bar{t}}$ and $\Delta\phi$ are predicted to be zero and π, respectively, because no transverse momentum exists at the initial collision. If these values are far from the predicted values, this may indicate an incorrect matching choice that is caused by combinatoric ambiguities. We also consider the distances (ΔR) between the reconstructed

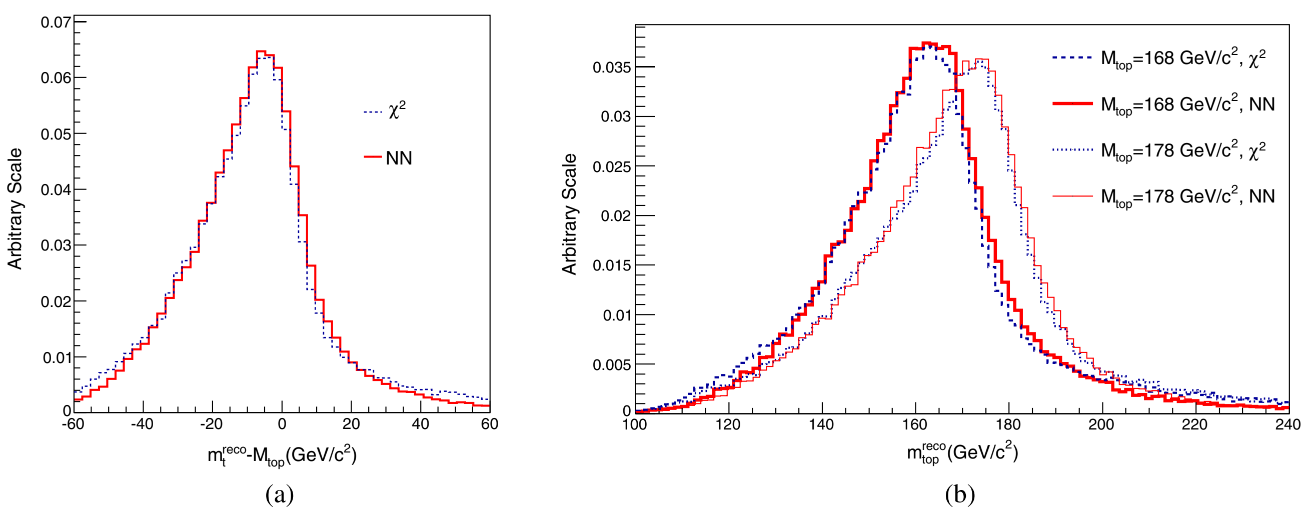

FIG. 4 (color online). (a) The m_t^{reco} minus $\mathrm{M_{top}}$ distributions of the $t\bar{t}$ sample using NN method (solid line) and the χ^2 method (dashed line) with $\mathrm{M_{top}} = 173\ \mathrm{GeV}/c^2$ are shown. The NN method has Better resolution (close to zero). (b) The m_t^{reco} distributions of the 168 GeV/c^2 $t\bar{t}$ sample using the NN method (thick solid line) and the χ^2 method (thick dotted line), and the 178 GeV/c^2 $t\bar{t}$ sample using the NN method (thin solid line) and the χ^2 method (thin dotted line) are presented. The NN method has better separation between the 168 GeV/c^2 and 178 GeV/c^2 samples.

particles, which are useful for determining the correct matching choice. The NN training input variables are listed below:

(1) χ^2: χ^2 value of the kinematic reconstruction.
(2) $p_T^{t\bar{t}}$: transverse momentum of the $t\bar{t}$ system.
(3) $\Delta\phi$: azimuthal angle between the t and $\bar{t}$ quarks.
(4) ΔR: distance between the t and $\bar{t}$ quarks.
(5) $\Delta R_{lW,lb}$: distance between the b quark and W boson of the leptonically decaying t quark.
(6) $\Delta R_{hW,hb}$: distance between the b quark and W boson of the hadronically decaying t quark.
(7) ΔR_{jj}: distance between the two jets of the hadronically decaying W boson.
(8) $\Delta R_{lt,lW}$: distance between the leptonically decaying t quark and its decaying daughter W boson.
(9) $\Delta R_{ht,hW}$: distance between the hadronically decaying t quark and its decaying daughter W boson.
(10) $\Delta R_{hW,q1}$: distance between the hadronically decaying W boson and its decaying daughter quark(1).
(11) $\Delta R_{hW,q2}$: distance between the hadronically decaying W boson and its decaying daughter quark(2).
(12) $\Delta R_{l,lb}$: distance between the lepton and b quark of the leptonically decaying t quark.
(13) $\Delta R_{b\bar{b}}$: distance between the b and $\bar{b}$ quark.

The distributions and the separation power of the input variables used in the NN for both the signal and the

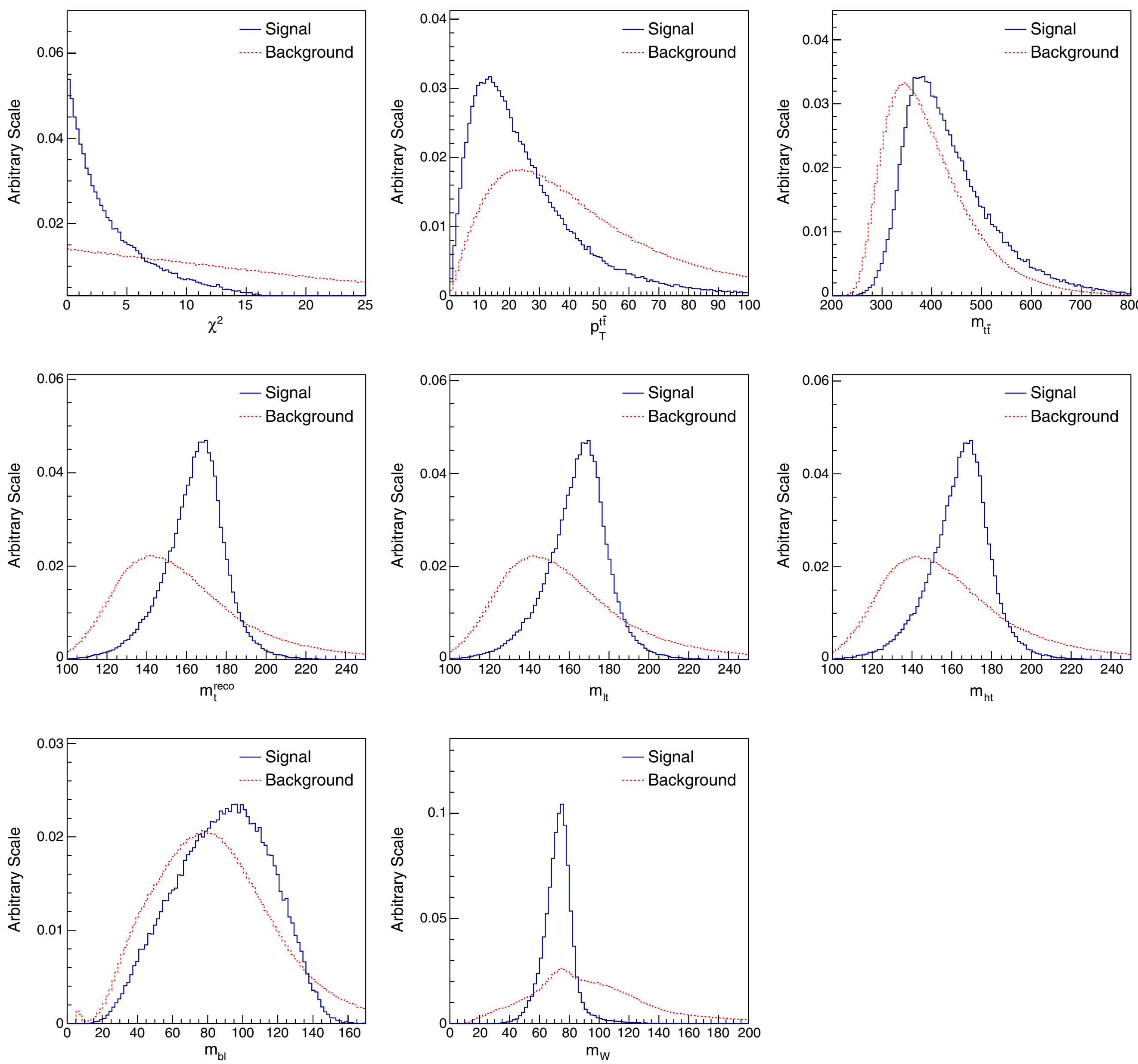

FIG. 5 (color online). Distributions of the neural network input variables for the A_{FB} measurement of the signal (all jets are correctly matched) and the background (at least one jet unmatched) using a SM $t\bar{t}$ sample with $M_{top} = 173\ \mathrm{GeV}/c^2$.

background are shown in Fig. 1. Even though χ^2 is useful for determining the correct matching, all of the other variables also provide meaningful discrimination between the signal and the background. Our NN configuration has twelve input variables, two hidden layers, and one output node. After training, we process the SM $t\bar{t}$ sample using the trained NN. Figure 2 shows the NN output value (NN_{out}) of the signal and the background. We find that NN_{out} produces a good separation power between the signal and the background.

In the χ^2 method, a candidate for the correct matching combination is chosen by the case that has the minimum χ^2 value. However, in the NN method, we choose the combination with the maximum NN_{out}. Because CDF analysis usually rejects poorly reconstructed events by requiring $\chi^2 < 9$, we also try to remove poorly reconstruction events in the NN method using maximum NN_{out} requirements. The purity of an event reconstruction is highly dependent on a fraction of the event passing the criteria (efficiency). We therefore study the relationship between the purity and the efficiency using each reconstruction method. Figure 3 shows the efficiency as a function of the purity for both the χ^2 method and the NN method. As we can see, the NN method has much higher purity for the same efficiency. If we select 76% efficiency in the NN method, which corresponds to an efficiency of $\chi^2 < 9$ in the χ^2 method, the NN_{out} criteria should be $NN_{out} > 0.60$. With this condition, the NN method has 47% purity, which is approximately 21% better than the χ^2 method.

For realistic M_{top} measurements, we study the reconstructed top-quark mass (m_t^{reco}) distribution, which is an observable of the M_{top} measurement [26]. We first examine the difference between the m_t^{reco} and the true M_{top} value of the SM $t\bar{t}$ sample. Figure 4(a) shows the distributions of m_t^{reco} minus M_{top} using two different reconstruction methods. As we can see, the NN method has better resolution (10%) than the χ^2 method. To study any bias on M_{top} in the NN reconstruction, we generate two additional SM $t\bar{t}$ samples that have different M_{top} values (168 GeV$/c^2$ and 178 GeV$/c^2$). We apply the NN trained by the $M_{top} = 173$ GeV$/c^2$ sample to both samples and compare the m_t^{reco} distributions. As shown in Fig. 4(b), the m_t^{reco} distribution is slightly smaller using the NN method. However, the mean value changes from the different mass samples are quite similar between the χ^2 method and the NN method. To quantify the performance, we calculate Δm_t^{reco}(178–168 GeV$/c^2$)/rms, where rms is average root-mean-square of the m_t^{reco} distributions. We obtain an approximately 11% higher value using the NN method than that of χ^2 method. Therefore, we can achieve better precision of the M_{top} measurement using the NN method with a quantitatively similar improvement in the statistical uncertainty.

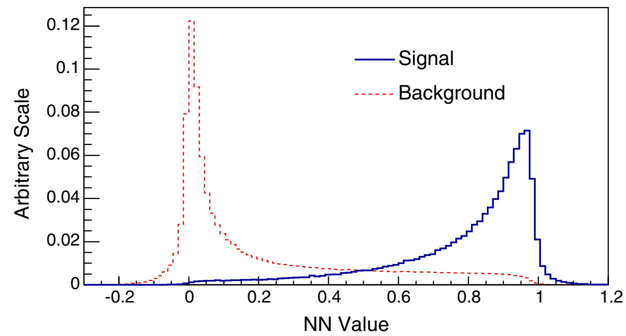

FIG. 6 (color online). Distribution of the neural network output for the A_{FB} measurement of the signal and the background using a SM $t\bar{t}$ sample with $M_{top} = 173$ GeV$/c^2$.

IV. A_{FB} MEASUREMENT

For the A_{FB} measurement, we consider kinematic variables that do not depend on the θ angle. We therefore do not consider the angles between particles. Because M_{top} is very precisely measured [12,13], we assume $M_{top} = 173$ GeV$/c^2$ is appropriate for A_{FB} measurements. With this assumption, the reconstructed masses of the particles are useful for denoting the correct combination. In general, incorrect combinations will yield smaller reconstructed masses as well as poorer resolutions. The full list of input variables for the A_{FB} measurement are shown below:

(1) χ^2: χ^2 value of the kinematic reconstruction.
(2) $p_T^{t\bar{t}}$: transverse momentum of the $t\bar{t}$ system.
(3) $m^{t\bar{t}}$: reconstructed invariant mass of the $t\bar{t}$ system.
(4) m_t^{reco}: reconstructed top-quark mass.
(5) m_{lt}: reconstructed mass of the leptonically decaying t quark.

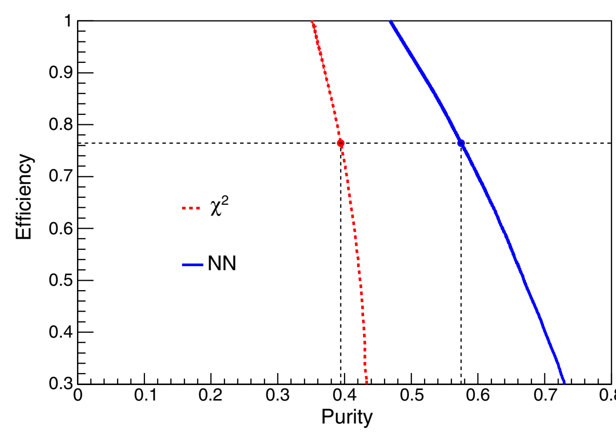

FIG. 7 (color online). The relationship between the purity and the efficiency of the NN method and the χ^2 method is shown. At the same efficiency (76%), which corresponds to the $\chi^2 < 9$ cut, the NN method has 57% purity, while the χ^2 method has 39% purity.

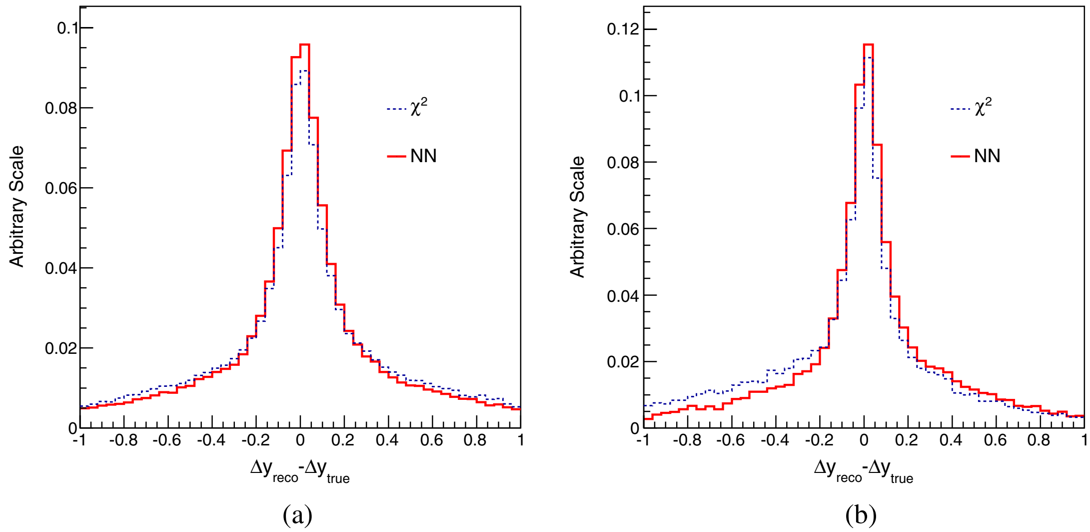

FIG. 8 (color online). The Δy_{reco} minus Δy_{true} distributions of the (a) SM $t\bar{t}$ sample and the (b) axigluon sample are shown using the NN method (solid line) and the χ^2 method (dashed line). In both models, NN method has better resolution.

(6) m_{ht}: reconstructed mass of the hadronically decaying t quark.
(7) m_{bl}: reconstructed invariant mass of the b quark and lepton in the leptonically decaying t quark.
(8) m_W: reconstructed mass of the hadronically decaying W boson.

The distributions and separation power of the input variables used in the NN for both the signal and the background are shown in Fig. 5. As we can see, the invariant masses of the reconstructed particles are very good discriminants. Our NN configuration for the A_{FB} measurement has eight input variables, two hidden layers, and one output node. After training, we process the SM $t\bar{t}$ sample with the trained NN. Figure 6 shows $\mathrm{NN}_{\mathrm{out}}$ for the signal and the background using the SM sample. We achieve a very good separation between the signal and the background. We also apply the NN method to select the maximum $\mathrm{NN}_{\mathrm{out}}$ combination.

We show the purity as a function of the efficiency in Fig. 7 for both the χ^2 method and the NN method. We obtain the $\chi^2 < 9$ efficiency when $\mathrm{NN}_{\mathrm{out}} > 0.58$. In this condition, we obtain 57% purity with the NN method, which is approximately 46% better than the χ^2 method.

In the measurement of A_{FB}, the reconstructed rapidity difference between t and $\bar{t}$ ($\Delta y = y_t - y_{\bar{t}}$) are widely used [6–8,30]. We investigate the reconstructed Δy (Δy_{reco}) using the NN method as well as the χ^2 method to verify the effectiveness of the reconstruction method for real measurements. Figure 8(a) shows Δy_{reco} minus the true Δy (Δy_{true}) of the SM $t\bar{t}$ sample. As we can see, the NN method has better resolution, which is approximately 9% better than that of the χ^2 method.

Because A_{FB} is approximately zero in the $t\bar{t}$ production of the LO SM process, we generate new physical processes with any significant A_{FB} value. Based on interesting models used to explain Tevatron A_{FB} results, we use the axigluon [31] (with 3 TeV/c^2 mass) mediated top-quark production. To generate the axigluon model, we use the MADGRAPH/MADEVENT package with the top-BSM model [32]. We apply the NN trained by the SM $t\bar{t}$ sample and examine the Δy distributions. As shown in Fig. 8(b), $\Delta y_{\mathrm{reco}} - \Delta y_{\mathrm{true}}$ does not shift with the NN method. In this sample, the true A_{FB} is 0.57. We can also see that the NN method has the better resolution, approximately 11%, for the Δy_{reco} distribution. Therefore, we can clearly improve A_{FB} measurements at Tevatron using the NN method instead of the χ^2 method.

V. SUMMARY AND CONCLUSION

In this paper, we investigate the feasibility of using an artificial NN to resolve combinatorial issues in the $t\bar{t}$ events at the hadron collider. We concentrated on the lepton + jets decay topology, where the four reconstructed jets should be matched with the four initial quarks. By including several input variables in the NN training, we have obtained very good discrimination between the signal and the background from $\mathrm{NN}_{\mathrm{out}}$. We then developed a reconstruction method based on $\mathrm{NN}_{\mathrm{out}}$. We have compared this method with the χ^2 method and improved the purity by 21% and 46% for the $\mathrm{M}_{\mathrm{top}}$ and A_{FB} measurements, respectively, without compromising the efficiency. We also present the reconstructed $\mathrm{M}_{\mathrm{top}}$ and Δy distributions for the $\mathrm{M}_{\mathrm{top}}$ and A_{FB} measurements, respectively. The NN does not introduce any additional bias compared with that of the χ^2 method, but the resolutions of the reconstructed variables are significantly improved. We therefore conclude that the NN method can improve the precision of important top-quark measurements such as M_{top} and A_{FB}. We plan to revisit this method using a full detector simulation with experimental groups.

The technique discussed in this paper is highly model dependent. However, multivariable techniques for performing event reconstruction can be applied to both well-known SM process measurements and to beyond Standard Model (BSM) process measurements if we have well-developed benchmark models. From this point of view, the technique discussed in this paper can be a very powerful tool for resolving combinatoric ambiguities at the hadron collider.

ACKNOWLEDGMENTS

This research was supported by the Basic Science Research Program through the National Research Foundation of Korea (NRF) funded by the Ministry of Education (NRF-2011-35B-C00007).

[1] F. Abe *et al.* (CDF Collaboration), Phys. Rev. Lett. **74**, 2626 (1995); S. Abachi *et al.* (D0 Collaboration), Phys. Rev. Lett. **74**, 2632 (1995).

[2] J. Beringer *et al.* (Particle Data Group), Phys. Rev. D **86**, 010001 (2012).

[3] M. Perelstein, M. E. Peskin, and A. Pierce, Phys. Rev. D **69**, 075002 (2004).

[4] G. Bhattacharyya, Rep. Prog. Phys. **74**, 026201 (2011).

[5] T. Aaltonen *et al.* (CDF Collaboration), Phys. Rev. Lett. **110**, 121802 (2013); V. M. Abazov *et al.* (D0 Collaboration), Phys. Rev. D **85**, 051101 (2012); G. Aad *et al.* (ATLAS Collaboration), Phys. Rev. D **88**, 012004 (2013); S. Chatrchyan *et al.* (CMS Collaboration), Phys. Rev. Lett. **111**, 211804 (2013).

[6] T. Aaltonen *et al.* (CDF Collaboration), Phys. Rev. D **83**, 112003 (2011).

[7] V. M. Abazov *et al.* (D0 Collaboration), Phys. Rev. D **84**, 112005 (2011).

[8] T. Aaltonen *et al.* (CDF Collaboration), Phys. Rev. D **87**, 092002 (2013).

[9] ALEPH, CDF, D0, DELPHI, L3, OPAL, SLD, LEP Electroweak Working Group, Tevatron Electroweak Working Group, and SLD Electroweak and Heavy Flavor Working Groups, arXiv:1012.2367v2.

[10] H. Flächer, M. Goebel, J. Haller, A. Hoecker, K. Mönig, and J. Stelzer, Eur. Phys. J. C **60**, 543 (2009).

[11] G. Aad *et al.* (ATLAS Collaboration), Phys. Lett. B **716**, 1 (2012); S. Chatrchyan *et al.* (CMS Collaboration), Phys. Lett. B **716**, 30 (2012).

[12] T. Aaltonen *et al.* (CDF and D0 Collaborations), arXiv: 1305.3929.

[13] CMS and ATLAS Collaborations, Report Nos. CMS-PAS-TOP-13-005 and ATLAS-CONF-2013-102.

[14] T. Aaltonen *et al.* (CDF Collaboration), Phys. Rev. D **73**, 032003 (2006).

[15] B. Abbott *et al.* (D0 Collaboration), Phys. Rev. D **58**, 052001 (1998).

[16] G. Aad *et al.* (ATLAS Collaboration), Eur. Phys. J. C **72**, 2046 (2012).

[17] S. Chatrchyan *et al.* (CMS Collaboration), J. High Energy Phys. 12 (2012) 105.

[18] J. Alwall, K. Hiramastsu, M. M. Nojiri, and Y. Shimizu, Phys. Rev. Lett. **103**, 151802 (2009).

[19] A. Rajaraman and F. Yu, Phys. Lett. B **700**, 126 (2011).

[20] P. Baringer, K. Kong, M. McCaskey, and D. Noonan, J. High Energy Phys. 10 (2011) 101.

[21] B. Denby, Comput. Phys. Commun. **119**, 219 (1999).

[22] L. Teodorescu, *Proceedings of Inverted CERN School of Computing 13, Geneva, 2008*.

[23] J. Alwall, P. Demin, S. de Visscher, R. Frederix, M. Herquet, F. Maltoni, T. Plehn, D. L Rainwater, and T. Stelzer, J. High Energy Phys. 09 (2007) 028.

[24] T. Sjostrand, P. Edén, C. Friberg, L. Lönnblad, G. Miu, S. Mrenna, and E. Norrbin, Comput. Phys. Commun. **135**, 238 (2001).

[25] J. Conway *et al.*, http://www.physics.ucdavis.edu/~conway/research/software/pgs/pgs4-general.htm.

[26] T. Aaltonen *et al.* (CDF Collaboration), Phys. Rev. D **79**, 092005 (2009); T. Aaltonen *et al.* (CDF Collaboration), Phys. Rev. D **83**, 111101 (2011); T. Aaltonen *et al.* (CDF Collaboration), Phys. Rev. Lett. **109**, 152003 (2012).

[27] T. Aaltonen *et al.* (CDF Collaboration), Phys. Rev. Lett. **108**, 151803 (2012); V. M. Abzov *et al.* (D0 Collaboration), Phys. Rev. Lett. **108**, 0151804 (2012).

[28] R. Brun and F. Rademakers, *Proceedings AIHENP'96 Workshop, Lausanne, 1996*; Nucl. Instrum. Methods Phys. Res., Sect. A **389**, 81 (1997); See also http://root.cern.ch.

[29] S. Choi and H. S. Lee, Phys. Rev. D **87**, 034012 (2013).

[30] G. Aad *et al.* (ATLAS Collaboration), J. High Energy Phys. 02 (2014) 107.

[31] P. H. Frampton and S. L. Glashow, Phys. Lett. B **190**, 157 (1987); J. Bagger, C. Schmidt, and S. King, Phys. Rev. D **37**, 1188 (1988).

[32] R. Frederix and F. Maltoni, J. High Energy Phys. 1 (2009) 047.